Physics of the Earth and Planetary Interiors 186 (2011) 191–197

Contents lists available at ScienceDirect

Physics of the Earth and Planetary Interiors

journal homepage: www.elsevier.com/locate/pepi

Short communication

Geomagnetic field intensity behavior in South America between 400 AD and 1800 AD: First archeointensity results from Argentina

Avto Goguitchaichvili [a,*], Catriel Greco [b], Juan Morales [a]

[a] Laboratorio Interinstitucional de Magnetismo Natural (LIMNA), Instituto de Geofísica, Unidad Michoacán, Universidad Nacional Autónoma de México, Campus Morelia 58190, Mexico
[b] CONICET – Museo Etnográfico J.B. Ambrosetti, Universidad de Buenos Aires, Argentina

ARTICLE INFO

Article history:
Received 9 September 2010
Received in revised form 10 March 2011
Accepted 20 March 2011
Available online 31 March 2011
Edited by: Keke Zhang

Keywords:
Archeomagnetism
Absolute geomagnetic intensity
Ceramics
South America
Argentina
Climate changes

ABSTRACT

An absolute archeointensity study in Northwest Argentina provided 25 independent geomagnetic field lectures supported by 37 radiometric dates between AD 400 and 1800. The mean, cooling rate and remanence anisotropy corrected archeointensity values obtained in this study range from 36.5 ± 2.6 to 63.1 ± 8.7 μT, with corresponding Virtual Axial Dipole Moments (VADMs) from 7.4 ± 0.5 to 12.7 ± 1.8 (10^{22} Am^2). Most of the data are concentrated between a relatively narrow interval from 1350 AD to 1550 AD. Three general features may be detected: the time intervals from about AD 1150 to 1350 and 1450 to 1600 are characterized by quite monotonic decay of geomagnetic intensity while some increase is observed from AD 1600 to 1700. The archeointensity decrease from about 17th century seems to be a general characteristic of global geomagnetic field because it was observed at different places worldwide. In the absence of reliable climate variation record for South America it is delicate to make any firm conclusions about the relationship between the Earth's magnetic field and multi-decadal climatic events. However, it is probably not a coincidence that persistent warm climate detected from Patagonia during AD 1200 to 1350 is consistent to geomagnetic intensity decrease revealed in this study.

1. Introduction

The fluctuations in geomagnetic field intensity may bring information on magneto-hydrodynamic processes acting in the core and core-mantle boundary. The variations of the geomagnetic field observed at Earth's surface can reveal many physical processes acting in the deep interiors of our planet. Recent archeomagnetic results also suggest a connection between the geomagnetic field and climatic changes during the Holocene (Gallet et al., 2006, 2008; Courtillot et al., 2007). The validation of this important and debated hypothesis definitively requires a better knowledge of the behavior of the geomagnetic field at different regions.

The geographic distribution of archeointensity data is still uneven (Genevey et al., 2008). In particular, very few data are available from the southern hemisphere (only ~5% of total data) which impedes an accurate analysis of the fine-scale changes in the statistical characteristics of paleosecular variation (Hartmann et al., 2010). Despite the impressive cultural heritage and abundant archaeological sites which makes this region a favorable place to obtain detailed records of the variation of the Earth's magnetic field during historical time, absolute geomagnetic intensity data are still very sparse.

We present in this paper new absolute geomagnetic intensity data from Rincon Chico (Northern Argentina) archeological site providing 25 independent geomagnetic field lectures supported by 37 radiometric dates. There is probably no other single archeological site in the world yielding such a large number of C^{14} ages and associated absolute intensities and it can be said that in this respect the Rincon Chico is a unique feature.

2. Archeological context and samples

The archaeological site Rincon Chico is located in the middle sector of the Santa Maria Valley in Catamarca province, northwestern Argentina (Fig. 1). With an area of 500 ha, it consists of 37 constructive units showing a pattern of settlement divided into three main areas: (a) a village conglomerate with at least 365 structures (mainly walls) located on the hill and the slopes of Sierra del Cajon; (b) 26 architectonical compounds located in different sectors of the site, and (c) areas of burials and places of specific activities such as agriculture and quarrying (Tarragó, 2007). The occupation of the locality, based on radiocarbon dating and relative chronological information from artifacts recovered during the excavations, continues during the period of Inca domination (about 1480–1536) and the Hispanic-Indigenous period until mid-17th century. The arrival of the Spaniards does not necessarily mean absolute control of the region, but more than a century of rebellions and alliances

* Corresponding author.
E-mail address: avto@geofisica.unam.mx (A. Goguitchaichvili).

0031-9201/$ - see front matter © 2011 Elsevier B.V. All rights reserved.
doi:10.1016/j.pepi.2011.03.007

Fig. 1. Schematic location map of Rincon Chico archeological site in the Santa Maria Valley (Catamarca province, northwestern Argentina). Also shown are: (a) bottom view of the village on the hillside. The walls of terraced housing structures are indicated with dotted lines. (band c) Closer look of some of these wall structures. (d and e) Archaeological excavations in housing and productive sectors of Rincón Chico. (f) Architectonic compound in the lower areas of the site. Invisible walls are with dashed lines. Bottom: Different types of vessels from Yocavil Valley.

between different ethnic groups against the invaders until the final domination (between 1659 and 1665 after Lorandi and Boixadós, 1988).

After more than 20 years of systematic research led by Dr. Myriam Tarragó, a fairly complete but also complex picture of the chronology of Rincón Chico is achieved. In total, 37 radiocarbon dates (Table 1) have been obtained (Tarragó, 2007) from the excavations in different sectors of the site (Fig. 1). Pottery samples studied here come from systematic excavations of the Rincón Chico archeological site. All samples were obtained in occupation layers of housing and productive sectors of the site. The study of different variables such as quantity, size, reassembly and stratigraphic distributions of fragments (Greco, 2007) helped to estimate the formation processes of ceramic assemblages. In addition, we carried out a detailed investigation of stylistic, technological and functional attributes. This allowed the almost direct association (following the criteria established by Waterbolk (1983)) of the radiocarbon dated events (hearths, charcoal concentrations and human burials) with the pottery.

We selected fragments that are stratigraphically (most of them unambiguously) associated with radiocarbon dates previously judged to be reliable (great details may be found in Greco, 2007). We note also that the pottery samples analyzed here correspond to both fine and coarse variants of the known Santa María ceramic style (see for example Weber, 1978), which also serves as an independent chronological marker *per se*.

3. Magnetic measurements

3.1. Rock-magnetic properties

Magnetic characteristics of typical samples selected for Thellier paleointensity measurements are summarized in Fig. 2 and could be described as follow:

1. Samples do not present a big capacity for viscous remanence acquisition. Viscosity experiments provided viscosity indexes generally less than 5%, which are small enough to obtain precise measurements of the remanence during the process of thermal demagnetization.
2. Low-field continuous susceptibility measurements performed in air (using a Bartington susceptibility meter MS2 equipped with furnace) show the presence of a single ferrimagnetic phase with Curie temperature compatible with Ti-poor titanomagnetite

Table 1
New mean Argentinian archeointensity data (summarized) and associated calibrated radiometric ages. n/N – Number of accepted samples for archeointensity determination/total number of analyzed pottery fragments.

Sample	Site	Laboratory code	Associated age (BP)	Intensity (mT)	VADM 10E22 (Am^2)	n/N
RCH1	Rincón Chico 1	Mean LP 1636 and 1638	600 ± 40	41.2 ± 0.6	8.3 ± 0.2	2/8
RCH2	Rincón Chico 1	LP 1426	490 ± 70	45.3 ± 2.7	9.1 ± 0.5	8/8
RCH3	Rincón Chico 1	Beta 131673	560 ± 70	50.3 ± 3.6	10.1 ± 0.7	7/8
RCH4	Rincón Chico 1	Beta 162369	630 ± 40	44.0 ± 5.4	8.9 ± 1.1	8/8
RCH6	Rincón Chico 1	LP 1622	570 ± 60	48.9 ± 7.4	9.6 ± 1.5	7/8
RCH7	Rincón Chico 1	LP 1350	310 ± 60	63.1 ± 8.7	12.7 ± 1.8	6/8
RCH9	Rincón Chico 1	LP 1656	770 ± ± 70	36.5 ± 2.6	7.4 ± 0.5	2/2
RCH11	Rincón Chico 1	LP 990	580 ± 80	37.1 ± 8.9	7.5 ± 1.8	6/8
RCH12	Rincón Chico 1	Beta 162380	240 ± 40	57.0 ± 5.2	11.4 ± 1.0	8/8
RCH16,17,18	Rincón Chico 12	Beta 130222	490 ± 50	52.8 ± 5.0	10.6 ± 1.0	16/18
RCH19	Rincón Chico 13	Beta 131674	560 ± 60	55.4 ± 6.2	11.3 ± 1.4	5/8
RCH20	Rincón Chico 14	LP 1015	430 ± 60	51.8 ± 7.7	10.4 ± 1.6	4/8
RCH22	Rincón Chico 15	LP 416	680 ± 110	49.2 ± 5.6	9.9 ± 1.1	8/8
RCH23	Rincón Chico 15	LP 416	680 ± 110	42.2 ± 4.9	8.5 ± 1.0	8/8
RCH25	Rincón Chico 15	LP 451	820 ± 80	49.7 ± 4.0	10.0 ± 0.8	8/10
RCH26	Rincón Chico 15	LP 392	890 ± 60	45.1 ± 1.9	9.1 ± 0.4	7/8
RCH27	Rincón Chico 15	Mean of various ages	590 ± 30	45.4 ± 2.0	9.1 ± 0.4	3/9
RCH28	Rincón Chico 15	Mean of various ages	590 ± 30	49.2 ± 4.7	9.9 ± 0.9	2/2
RCH29	Rincón Chico 15	LP 401	660 ± 70	47.5 ± 4.6	9.6 ± 0.9	8/9
RCH30,30bis	Rincón Chico 15	LP 728	570 ± 60	46.9 ± 1.5	9.5 ± 0.3	10/10
RCH31	Rincón Chico 15	LP 713	500 ± 60	49.9 ± 2.1	10.1 ± 0.4	9/9
RCH32	Rincón Chico 15	LP 401	660 ± 70	42.4 ± 4.6	8.5 ± 0.9	8/9
RCH34	Rincón Chico 15	LP 1461	650 ± 60	44.6 ± 3.7	8.9 ± 0.6	5/9
RCH35	Rincón Chico 15	LP 1021	210 ± 60	50.3 ± 4.5	10.1 ± 0.9	9/9
RCH36,37	Rincón Chico 18	Mean LP 428 and LP 471	960 ± 70	54.3 ± 3.2	10.9 ± 0.7	3/7

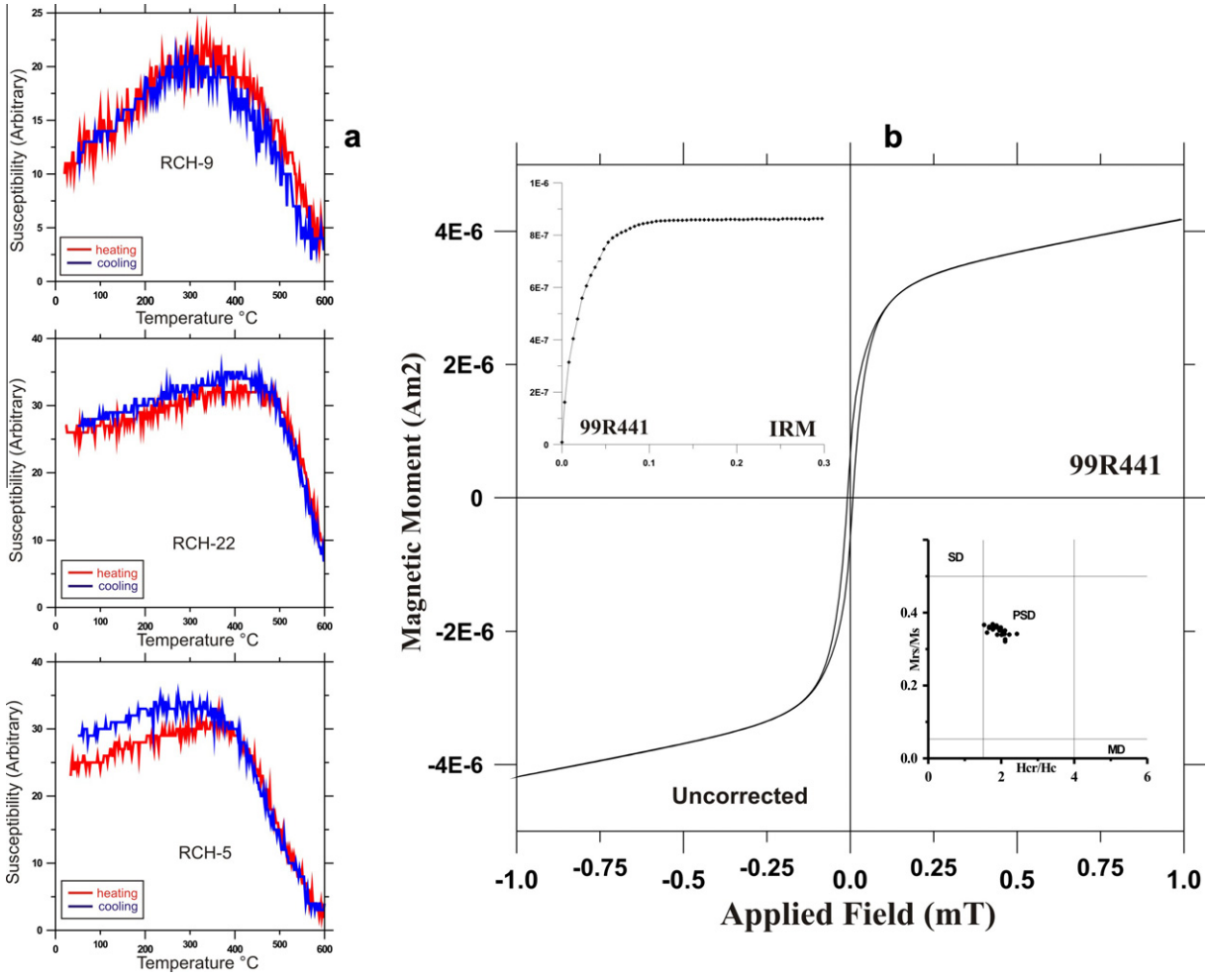

Fig. 2. Summary of rock-magnetic experiments: (a) susceptibility versus temperature curves for representative samples. Red (blue) branch corresponds to heating (cooling) curves, respectively. (b) Typical hysteresis loop (uncorrected for dia- and paramagnetism) and corresponding isothermal remanent magnetization curve. Also shown is a Day plot (Day et al., 1977). (For interpretation of the references to colour in this figure legend, the reader is referred to the web version of this article.)

(Fig. 2a). However, cooling and heating curves are not perfectly reversible probably due to the low sensitivity of the Bartington susceptibility system. However, these curves may be still used to determine the Curie temperatures of magnetic carriers and estimate their thermal stability – a decisive factor for archeointensity experiments. Curie points were determined taking inflexion points in curves following the drop of susceptibility corresponding to the destruction of ferromagnetic phases (Prévot et al., 1983). We obtained a relatively large interval of Curie temperatures ranging from 520 to 585 °C. These values are characteristic of Ti-poor titanomagnetites with variable titanium content.

3. Hysteresis measurements at room temperature were performed on all studied samples in fields up to 1.1 T using the AGFM 'Micromag' apparatus. The saturation remanent magnetization

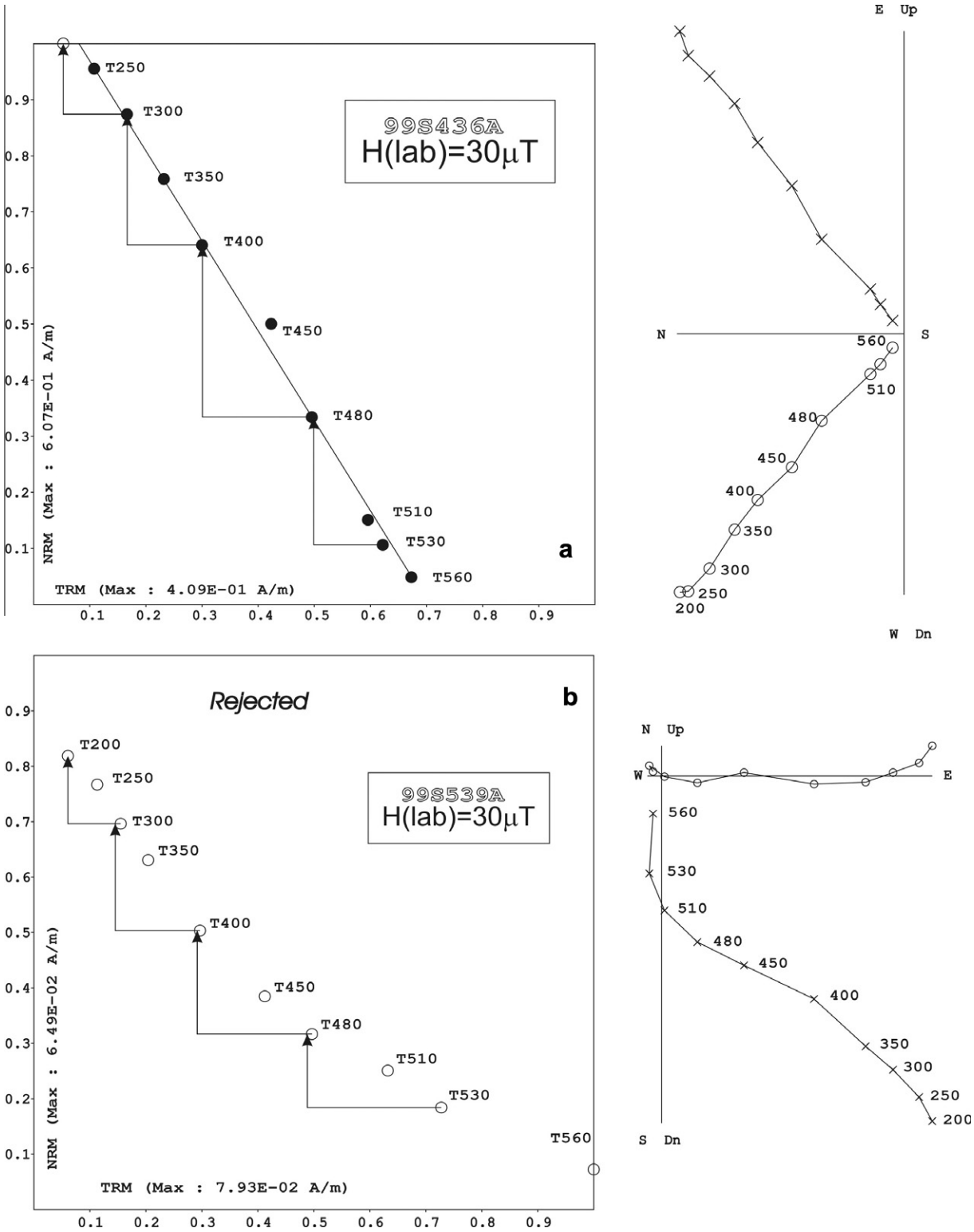

Fig. 3. Representative NRM–TRM plots and associated orthogonal vector demagnetization diagrams for the Rincon Chico samples. In the NRM–TRM plots, arrows refer to "pTRM" checks.

(J_{rs}), the saturation magnetization (J_s) and coercitive force (H_c) were calculated after correction for the paramagnetic contribution. The coercivity of remanence (H_{cr}) was determined by applying a progressively increasing backfield after saturation. A representative curve is shown in Fig. 2b together with the associated isothermal remanence acquisition graph and Day et al. (1977) diagram. For most samples, 'small' pseudo-single-domain grains seem to be responsible for remanence judging from hysteresis parameters values (Dunlop, 2002). Same author suggests that this behavior may due to the mixture of single domain (mostly) and multi domain magnetic grains which is our preferred interpretation.

3.2. Archeointensity determinations

Archeointensity experiments were performed using the Thellier method (Thellier and Thellier, 1959) in its modified form (Coe, 1967) on 207 samples (please see Supplementary material at www.geofisica.unam.mx/RinconChico. Heating and cooling were made in air, and the laboratory field was set to 30 μT. Ten temperature steps were distributed between room temperature and 560 °C and several control heatings (i.e. reinvestigations of results from previous heating steps, commonly referred to as partial TRM (pTRM) checks) were performed throughout the experiments).

Cooling rate dependence of TRM was investigated following a modified procedure described in Chauvin et al. (2000). TRM gained during last step of the Thellier experiment (560 °C) was subsequently designated as TRM1. At the same temperature, a new full TRM (TRM2) was given to all samples but this time using a long cooling time (~6–7 h). Finally, a third TRM (TRM3) was created using the same cooling time (of about 45 min) as that used to create TRM1. The effect of cooling rate upon TRM intensity was estimated by calculating the percentage variation between the intensity acquired during a short and a long cooling time (TRM1 and TRM2). The cooling rate effect is calculated as the difference between the fast and slow cooling time acquired magnetizations. It is expressed in percentage as TRM (%) = TRM1−TRM2/TRM1 (%). Changes in TRM acquisition capacity were estimated by means

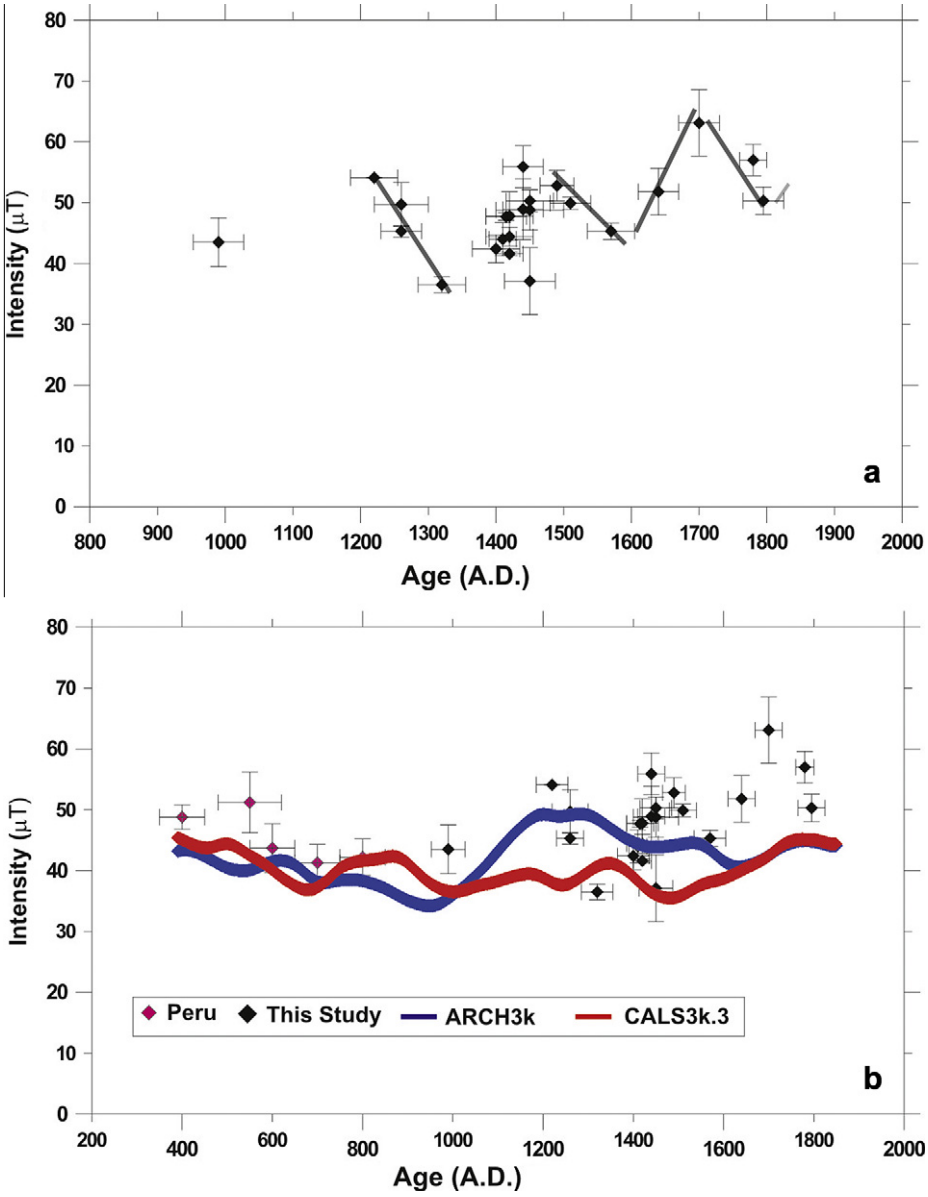

Fig. 4. (a) Mean archeointensities retrieved from Rincon Chico archeological site against calibrated C^{14} ages. (b) Currently available absolute intensity data from Northern Argentina and Peru (this study and Shaw et al. (1996)). Also shown are the data derived from the CALS3k.3 and ARCH3K model prediction (Donadini et al., 2009).

of the percentage variation between the intensity acquired during same cooling time (TRM1 and TRM3). Cooling rate correction was applied only when the corresponding change in TRM acquisition capacity was below 15%.

The magnetic anisotropy effect has been estimated by determining the TRM anisotropy tensor for all samples. ATRM measurements have been carried out by inducing a pTRM (560 °C to room temperature) in six sample directions (i.e. $+x$, $+y$, $+z$, $-x$, $-y$, $-z$). Subsequent to this sequence, a stability check was made by repeating a pTRM acquisition again in the $+x$ direction. Zero field thermal demagnetizations at 560 °C before each pTRM were used as a baseline (Tema et al., 2010). It should be noted that for the thermally altered samples (judging from the changes in TRM acquisition capacity during the cooling rate experiments) no TRM anisotropy correction was applied.

As should be expected the cooling rate and anisotropy corrections significantly reduced the standard deviation of the mean intensities, suggesting the importance of such a correction in this kind of study. The site-mean archeointensity values obtained in this study before cooling rate and anisotropy corrections range from 41.6 ± 4.3 to 69.6 ± 11.2 μT while corrected values provided 36.5 ± 2.6 to 63.1 ± 8.7 μT, respectively.

4. Main results and discussion

Archeointensity data are reported on the classical NRM–TRM plot (so called Arai–Nagata curves) on Fig. 3 while results of individual sample are given as Supplementary material and summarized results are provided in Table 1. We accepted only determinations: (1) which were obtained from at least five NRM–TRM points corresponding to a NRM fraction larger than 1/3 and (2) yielding a quality factor (Coe et al., 1978) of about 5 or more. These samples are characterized by long linear segments and positive pTRM checks. NRM end point directions are also linear and point to the origin (Fig. 3a). Samples exhibiting nonlinear trend (e.g. a high dispersion or a concave behavior) were rejected for further analysis (e.g. Fig. 3b).

One hundred and sixty-seven samples (out of 207 analyzed) fulfill the above described basic criteria and definitively correspond to high technical standards. The site-mean archeointensity values obtained in this study range from 36.5 ± 2.6 to 63.1 ± 8.7 μT, with corresponding Virtual Axial Dipole Moments (VADMs) from 7.4 ± 0.5 to 12.7 ± 1.8 (10^{22} Am^2). The Rincon Chico mean archeointensities are shown on Fig. 4a against calibrated radiometric dates (A.D.). The record consists of 25 mean archeointensities distributed between 900 AD and 1800 AD. The data set shows several distinct periods of quite large intensity fluctuations. However, most data are concentrated between a relatively narrow interval from 1350 AD to 1550 AD. Three general features may be detected: the time interval from about AD 1150 to 1350 and 1450 to 1600 are characterized by quite monotonic decrease of geomagnetic intensity while some increase is observed from AD 1600 to 1700. As suggested by Gallet et al. (2005) and Courtillot et al. (2007) these fluctuations may be correlated to climate changes over multi-decadal time scales. The cooling (warming) episodes at least at North Atlantic are synchronous to the intensity increase (decrease) and seem to be influenced by geomagnetic field trough the modulation of cosmic ray flux interacting with the atmosphere. It is hard to make any firm conclusions about this relationship in the absence of reliable climate variation record for South America. It is however probably not a coincidence that persistent warm climate detected from Patagonia (Stine, 1994) during AD 1200–1350 is consistent with geomagnetic intensity decrease revealed in this study. The archeointensity decay from about 17th century seems to be a general characteristic of global geomagnetic field because it was observed at different places worldwide (Valet et al., 2008; Gómez-Paccard et al., 2006; Genevey et al., 2009; Hartmann et al., 2010).

Donadini et al. (2009) recently produced a series of time-varying spherical harmonic models of the geomagnetic field for the last 3000 years based on a new compilation of lake sediment records and the GEOMAGIA50v2 online database. The SED3K model is based on lake sediment records while the data coming from archeological artifacts and lavas are involved to construct the ARCH3K curves. The new CALS3k.3 model uses all available measurements from sediments, lavas and archeological structures and currently provides the best global representation of the 0–3 ka field. Most of the currently available, reliable archeointensity data (Fig. 4b) from western South America (this study and data from Shaw et al., 1996) agree within some uncertainties with ARCH3K model prediction between 400 AD and 1550 AD. However, the general decrease of absolute intensity from 17th century is not observed. As suggested by Donadini et al. (2009), the ARCH3K may work better for the sites out of Western Europe.

Acknowledgments

This work was supported by the Mexican Science Foundation, CONACyT grants # 54957 and 129653. The photos at Figure 1 (different types of vessels from Yocavil Valley, stored at E. Boman Museum, Santa Maria) are taken by V. Palamarczuk.

Appendix A. Supplementary data

Supplementary data associated with this article can be found, in the online version, at doi:10.1016/j.pepi.2011.03.007.

References

Chauvin, A., Garcia, A., Lanos, Ph., Laubenheimer, F., 2000. Paleointensity of the geomagnetic field recovered on archaeomagnetic sites from France. Phys. Earth Planet. Int. 120, 111–136.

Coe, R.S., 1967. Paleo-intensities of the Earth's magnétic field determined from tertiary and quaternary rocks. J. Geophys. Res. 72 (12), 3247–3262.

Coe, R.S., Grommé, S., Mankinen, E.A., 1978. Geomagnetic paleointensities from radiocarbon-dated lava flows on Hawaii and the question of the Pacific nondipole low. J. Geophys. Res. 83 (B4), 1740–1756.

Courtillot, V., Gallet, Y., Le Mouël, J.-L., Fluteau, F., Genevey, A., 2007. Are there connections between the Earth's magnetic field and climate? Earth Planet. Sci. Lett. 253, 328–339.

Day, R., Fuller, M., Schmidt, V.A., 1977. Hysteresis properties of titanomagnetites: grain-size and compositional dependence. Phys. Earth Planet. Int. 13, 206–267.

Donadini, F., Korte, M., Constable, C.G., 2009. Geomagnetic field for 0–3 ka: 1. New data sets for global modeling. Geochem. Geophys. Geosyst. 10, Q06007. doi:10.1029/2008GC002295.

Dunlop, D.J., 2002. Theory and applications of the Day plot (Mra/Mr versus Hcr/Hc). Theorical curves and test using titanomagnetite data. J. Geophys Res. 107 (b3), 1029–2001.

Gallet, Y., Genevey, A., Fluteau, F., 2005. Does Earth's magnetic field secular variation control centennial climate change? Earth Planet. Sci. Lett. 236, 339–347.

Gallet, Y., Genevey, A., Le Goff, M., Fluteau, F., Eshraghi, S.A., 2006. Possible impact of the Earth's magnetic field on the history of ancient civilizations. Earth Planet. Sci. Lett. 246, 17–26.

Gallet, Y., Le Goff, M., Genevey, A., Margueron, J.C., Matthiae, P., 2008. Geomagnetic field intensity behavior in the Middle East between 3000 BC and 1500 BC. Geophys. Res. Lett. 35, L02307. doi:10.1029/2007GL031991.

Genevey, A., Gallet, Y., Constable, C.G., Korte, M., Hulot, G., 2008. ArcheoInt: an upgrated compilation of geomagnetic field intensity data for the past ten millennia and its application to the recovery of the past dipole moment. Geochem. Geophys. Geosyst. 9 (4), Q04038. doi:10.1029/2007/GC001881.

Genevey, A., Gallet, Y., Rosen, J., Le Goff, M., 2009. Evidence for rapid geomagnetic field intensity variations in Western Europe over the past 800 years from new archeointensity French data. Earth Planet. Sci. Lett. 284, 132–143.

Gómez-Paccard, M., Chauvin, A., Lanos, Ph., Thiriot, J., Jimenez-Castillo, P., 2006. Archeomagnetic study of seven contemporaneous kilns from Murcia (Spain). Phys. Earth Planet. Int. 157, 16–32.

Greco, C., 2007. Secuencias radiocarbónicas y estilos cerámicos en Rincón Chico, Valle de Yocavil, Catamarca. Universidad de Buenos Aires, Buenos Aires, p. 155.

Hartmann, G., Genevey, A., Gallet, Y., Trindade, R., Etchevarne, C., Le Goff, M., Afonso, M.C., 2010. Archeointensity in Northeast Brazil over the past five centuries. Earth Planet. Sci. Lett. 296 (3–4), 340–352.

Lorandi, A.M., Boixadós, R., 1988. Etnohistoria de los valles Calchaquíes en los siglos XVI y XVII. Runa XVII–XVIII, 263–419.

Prévot, M., Mainkinen, E.A., Grommé, S., Lecaille, A., 1983. High paleointensity of the geomagnetic field from thermomagnetic studies on rift valley pillow basalts from the middle Atlantic ridge. J. Geophys. Res. 88, 2316–2326.

Shaw, J., Walton, D., Yang, S., Rolph, T.C., Share, J.A., 1996. Microwave archaeintensities from Peruvian ceramics. Geophys. J. Int. 124, 241–244.

Stine, S., 1994. Extreme and persistent drought in California and Patagonia during medieval time. Nature 369, 546–549.

Tarragó, M., 2007. Ámbitos domésticos y de producción artesanal en el Noroeste Argentino prehispánico. Intersecciones Antropol. (8), 87–100.

Tema, E., Goguitchaichvili, A., Camps, P., 2010. Archaeointensity determinations from Italy: new data and the Earth's magnetic field strength variation over the past three millennia. Geophys. J. Int. 180, 596–608.

Thellier, E., Thellier, O., 1959. Sur l'intensité du champ magnétique terrestre dans le passé historique et géologique. Ann. Géophys. 15, 285–376.

Valet, J.P., Herrero-Bervera, E., Le Mouël, J.L., Plenier, G., 2008. Secular variation of the geomagnetic dipole during the past 2000 years. Geochem. Geophys. Geosyst. 9 (1), Q01008. doi:10.1029/2007GC001728.

Waterbolk, H.T., 1983. Ten guidelines for the archaeological interpretation of radiocarbon data. In: Proceedings of the First International Symposium C14 and Archaeology, Strasbourg, pp. 57–70.

Weber, R.L., 1978. A Seriation of the Late Prehistoric Santa Maria Culture of Northwerstern Argentina. Fieldiana Anthropol. 68 (2), 49–98.